NISSUNA UMANA INVESTIGAZIONE SI PUO DIMANDARE VERA SCIENZIA
S'ESSA NON PASSA PER LE MATEMATICHE DIMOSTRAZIONI
LEONARDO DA VINCI

vol. 6 no. 2 2018

MATHEMATICS AND MECHANICS of Complex Systems

XU WANG AND PETER SCHIAVONE

AN ARBITRARILY SHAPED ESHELBY INCLUSION INTERACTING WITH A CIRCULAR PIEZOELECTRIC INHOMOGENEITY PENETRATED BY A SEMI-INFINITE CRACK

msp

MATHEMATICS AND MECHANICS OF COMPLEX SYSTEMS
Vol. 6, No. 2, 2018
dx.doi.org/10.2140/memocs.2018.6.125

AN ARBITRARILY SHAPED ESHELBY INCLUSION INTERACTING WITH A CIRCULAR PIEZOELECTRIC INHOMOGENEITY PENETRATED BY A SEMI-INFINITE CRACK

XU WANG AND PETER SCHIAVONE

We study the interaction between an Eshelby inclusion of arbitrary shape and a circular piezoelectric inhomogeneity penetrated by a semi-infinite crack under antiplane mechanical and in-plane electrical loading in a linear piezoelectric solid. The Eshelby inclusion undergoes uniform antiplane eigenstrains and in-plane eigenelectric fields. Through the use of a conformal mapping, the cracked piezoelectric plane is first mapped onto the lower half of the image plane. The corresponding boundary value problem is then studied in this image plane. The interaction problem is solved through the construction of an auxiliary function and the application of analytic continuation across straight and circular boundaries. We obtain concise expressions for the resultant stress and electric displacement intensity factors at the crack tip.

1. Introduction

It is well-known that various kinds of defects, such as dislocations, cracks, Eshelby inclusions, and inhomogeneities can significantly affect the performance and integrity of piezoelectric devices. Theoretical analysis of these defects has continued to attract the attention of several researchers in the literature; see, for example, [Deeg 1980; Pak 1990; Kuo and Barnett 1991; Suo et al. 1992; Chung and Ting 1996; Lee et al. 2000; Ru 2000; 2001; Wang and Fan 2015; Wang and Schiavone 2017]. Ru [2000; 2001] used the technique of analytic continuation together with carefully constructed auxiliary functions in the physical plane to derive analytic solutions for Eshelby's problem of a two-dimensional Eshelby inclusion of arbitrary shape in a piezoelectric plane or half-plane or in one of two perfectly bonded piezoelectric half-planes. One example of the practical importance of Eshelby's problem lies in the study of residual stresses induced by lattice mismatch between buried active components and surrounding materials in strained semiconductor devices. It is

Communicated by David J. Steigmann.
MSC2010: 30E25, 74B05, 74G70.
Keywords: crack, Eshelby inclusion, inhomogeneity, piezoelectric material, analytic continuation, conformal mapping, field intensity factors.

well-known that these residual stresses crucially affect the electronic performance of these devices and may lead to failure and degradation [Ru 2000; 2001].

This work investigates the Eshelby inclusion problem in fibrous piezoelectric composites containing cracks. In this paper, we endeavor to consider, simultaneously, within one single framework, the effects of a crack, an inhomogeneity, and an Eshelby inclusion in piezoelectric materials. More specifically, we study the antiplane shear deformations of an infinite hexagonal piezoelectric matrix containing

(i) a circular hexagonal piezoelectric inhomogeneity partially penetrated by a semi-infinite crack, and

(ii) an Eshelby inclusion of arbitrary shape undergoing uniform antiplane eigenstrains and in-plane eigenelectric fields; when the matrix is subjected to remote antiplane mechanical and in-plane electrical loading.

The piezoelectric plane weakened by the semi-infinite crack is first mapped onto the lower half of an image plane constructed via the use of a conformal mapping. The corresponding problem is then studied in this image plane. The construction of a specific auxiliary function and the application of analytic continuation across straight and circular boundaries lead to the derivation of analytic vector functions in each of the three phases of the fibrous piezoelectric composite. The resultant field intensity factors at the crack tip are also obtained. Our analysis indicates that when a condition on eigenstrains and eigenelectric fields is met, the Eshelby inclusion will exert a neutral effect (neither shielding nor antishielding) on the electroelastic field at the crack tip.

2. Basic formulation

In the case of antiplane shear deformations of a hexagonal piezoelectric material with poling direction along the x_3-axis, the general solution can be expressed in terms of a two-dimensional analytic vector function $\boldsymbol{f}(z)$ of the complex variable $z = x_1 + i x_2$ as

$$\begin{bmatrix} \varphi_1 \\ \varphi_2 \end{bmatrix} + \mathrm{i}\boldsymbol{C} \begin{bmatrix} u_3 \\ \phi \end{bmatrix} = \boldsymbol{C}\boldsymbol{f}(z), \tag{1}$$

$$\begin{bmatrix} 2\varepsilon_{32} + 2\mathrm{i}\varepsilon_{31} \\ -E_2 - \mathrm{i}E_1 \end{bmatrix} = \boldsymbol{f}'(z), \qquad \begin{bmatrix} \sigma_{32} + \mathrm{i}\sigma_{31} \\ D_2 + \mathrm{i}D_1 \end{bmatrix} = \boldsymbol{C}\boldsymbol{f}'(z), \tag{2}$$

$$\boldsymbol{C} = \boldsymbol{C}^T = \begin{bmatrix} C_{44} & e_{15} \\ e_{15} & -\epsilon_{11} \end{bmatrix}, \tag{3}$$

where φ_1 and φ_2 are the stress function and charge potential, respectively; u_3 and ϕ are the antiplane displacement and electric potential, respectively; σ_{31} and σ_{32} are the antiplane shear stresses; D_1 and D_2 are electric displacements; E_1 and E_2

are in-plane electric fields; ε_{31} and ε_{32} are mechanical strains; C_{44}, e_{15}, and ϵ_{11} are the elastic, piezoelectric, and dielectric constants, respectively.

In addition, the stress function and the charge potential are defined in terms of the stresses and the electric displacements, respectively, by

$$\sigma_{31} = -\varphi_{1,2}, \quad \sigma_{32} = \varphi_{1,1}, \quad D_1 = -\varphi_{2,2}, \quad D_2 = \varphi_{2,1}. \tag{4}$$

3. An Eshelby inclusion near a cracked circular piezoelectric inhomogeneity

As shown in Figure 1, we consider an infinite hexagonal piezoelectric matrix containing an Eshelby inclusion of arbitrary shape undergoing uniform antiplane eigenstrains (ε^*_{31}, ε^*_{32}) and in-plane eigenelectric fields (E^*_1, E^*_2) as well as a circular hexagonal piezoelectric inhomogeneity. The poling directions of all three phases lie along the x_3-axis. A semi-infinite traction-free and charge-free crack partially penetrating the inhomogeneity lies on the negative real axis. The electroelastic constants of the matrix are identical to those of the inclusion but are different from those of the inhomogeneity. We represent the matrix by the domain S_2 and assume that the inhomogeneity occupies a circular region S_1 of radius R with its center at the origin. The inclusion is assumed to occupy the region denoted by S_3. Both the inhomogeneity-matrix interface $|z| = R$ and the inclusion-matrix interface denoted here by Γ are assumed to be perfectly bonded. Throughout the paper, the quantities in S_1, S_2, and S_3 will be identified by the subscripts 1, 2, and 3, respectively.

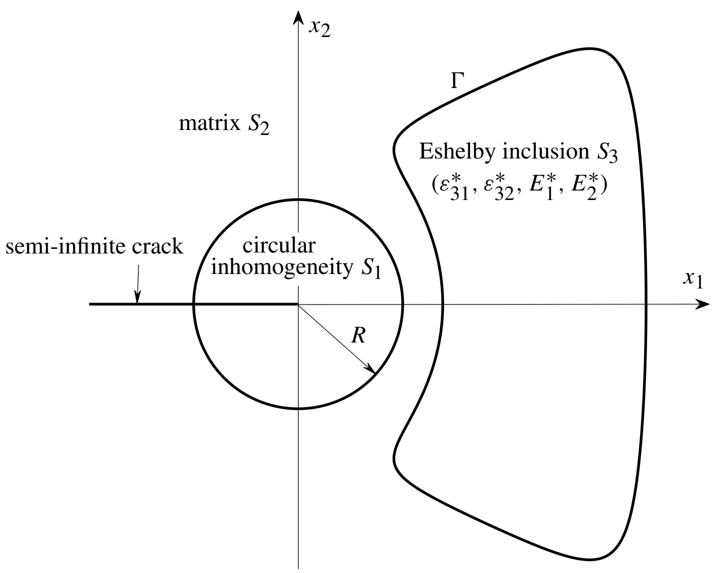

Figure 1. Interaction of an Eshelby inclusion of arbitrary shape with a circular piezoelectric inhomogeneity partially penetrated by a semi-infinite crack.

In the physical z-plane, the boundary value problem has the form

$$\begin{aligned} \boldsymbol{f}_1(z)+\overline{\boldsymbol{f}_1(z)}&=\mathbf{0}, \quad -R<x_1<0, \qquad x_2=0^{\pm};\\ \boldsymbol{f}_2(z)+\overline{\boldsymbol{f}_2(z)}&=\mathbf{0}, \quad -\infty<x_1<-R, \quad x_2=0^{\pm}; \end{aligned} \tag{5a}$$

$$\begin{aligned} \boldsymbol{C}_1\boldsymbol{f}_1(z)+\boldsymbol{C}_1\overline{\boldsymbol{f}_1(z)}&=\boldsymbol{C}_2\boldsymbol{f}_2(z)+\boldsymbol{C}_2\overline{\boldsymbol{f}_2(z)},\\ \boldsymbol{f}_1(z)-\overline{\boldsymbol{f}_1(z)}&=\boldsymbol{f}_2(z)-\overline{\boldsymbol{f}_2(z)}, \quad |z|=R; \end{aligned} \tag{5b}$$

$$\begin{aligned} \boldsymbol{f}_2(z)+\overline{\boldsymbol{f}_2(z)}&=\boldsymbol{f}_3(z)+\overline{\boldsymbol{f}_3(z)},\\ \boldsymbol{f}_2(z)-\overline{\boldsymbol{f}_2(z)}&=\boldsymbol{f}_3(z)-\overline{\boldsymbol{f}_3(z)}+\begin{bmatrix} 2(\varepsilon_{32}^*+\mathrm{i}\varepsilon_{31}^*)z-2(\varepsilon_{32}^*-\mathrm{i}\varepsilon_{31}^*)\bar{z}\\ -(E_2^*+\mathrm{i}E_1^*)z+(E_2^*-\mathrm{i}E_1^*)\bar{z} \end{bmatrix}, \quad z\in\Gamma; \end{aligned} \tag{5c}$$

$$\boldsymbol{f}_2(z)\cong\sqrt{2/\pi}\,\boldsymbol{C}_2^{-1}\boldsymbol{K}\sqrt{z}+O(1), \quad |z|\to\infty, \tag{5d}$$

where

$$\boldsymbol{K}=[K^{\sigma}\ K^{D}]^{T}, \tag{6}$$

in which K^{σ} and K^{D} denote the stress and electric displacement intensity factors, respectively. These intensity factors represent the far-field electromechanical loads.

Consider the following conformal mapping function:

$$z=\omega(\xi)=-\xi^2, \quad \xi=\omega^{-1}(z)=-\mathrm{i}\sqrt{z}, \quad \mathrm{Im}\{\xi\}\le 0. \tag{7}$$

The physical z-plane with the semi-infinite crack is mapped onto the lower half-ξ-plane and the crack faces are mapped onto the real axis in the ξ-plane. Moreover, the inhomogeneity $z\in S_1$ is mapped onto $\xi\in\Omega_1$; the matrix $z\in S_2$ is mapped onto $\xi\in\Omega_2$; the Eshelby inclusion $z\in S_3$ is mapped onto $\xi\in\Omega_3$; the inhomogeneity-matrix interface $|z|=R$ is mapped onto the semicircle $|\xi|=R^{1/2}$, $-\pi\le\arg\{\xi\}\le 0$; and, finally, the inclusion-matrix interface $z\in\Gamma$ is mapped onto $\xi\in L$ (see Figure 2).

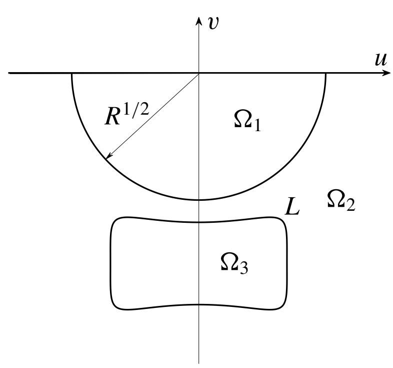

Figure 2. The problem in the ξ-plane.

Without loss of generality, we write $\boldsymbol{f}_i(\xi) = \boldsymbol{f}_i(\omega(\xi))$, $i = 1, 2, 3$ and denote by u and v the real and imaginary parts of ξ (i.e., $\xi = u + \mathrm{i}v$). In the image ξ-plane, the boundary value problem takes the form

$$\begin{aligned} \boldsymbol{f}_1(\xi) + \overline{\boldsymbol{f}_1(\xi)} &= \boldsymbol{0}, \qquad |u| < R^{1/2}, \qquad v = 0^-; \\ \boldsymbol{f}_2(\xi) + \overline{\boldsymbol{f}_2(\xi)} &= \boldsymbol{0}, \quad R^{1/2} < |u| < \infty, \quad v = 0^-; \end{aligned} \tag{8a}$$

$$\begin{aligned} &\boldsymbol{C}_1 \boldsymbol{f}_1(\xi) + \boldsymbol{C}_1 \overline{\boldsymbol{f}_1(\xi)} = \boldsymbol{C}_2 \boldsymbol{f}_2(\xi) + \boldsymbol{C}_2 \overline{\boldsymbol{f}_2(\xi)}, \\ &\boldsymbol{f}_1(\xi) - \overline{\boldsymbol{f}_1(\xi)} = \boldsymbol{f}_2(\xi) - \overline{\boldsymbol{f}_2(\xi)}, \quad |\xi| = R^{1/2}, \quad -\pi \le \arg\{\xi\} \le 0; \end{aligned} \tag{8b}$$

$$\begin{aligned} &\boldsymbol{f}_2(\xi) + \overline{\boldsymbol{f}_2(\xi)} = \boldsymbol{f}_3(\xi) + \overline{\boldsymbol{f}_3(\xi)}, \\ &\boldsymbol{f}_2(\xi) - \overline{\boldsymbol{f}_2(\xi)} = \boldsymbol{f}_3(\xi) - \overline{\boldsymbol{f}_3(\xi)} + \begin{bmatrix} -2(\varepsilon_{32}^* + \mathrm{i}\varepsilon_{31}^*)\xi^2 + 2(\varepsilon_{32}^* - \mathrm{i}\varepsilon_{31}^*)\bar{\xi}^2 \\ (E_2^* + \mathrm{i}E_1^*)\xi^2 - (E_2^* - \mathrm{i}E_1^*)\bar{\xi}^2 \end{bmatrix}, \quad \xi \in L; \end{aligned} \tag{8c}$$

$$\boldsymbol{f}_2(\xi) \cong \mathrm{i}\sqrt{2/\pi}\, \boldsymbol{C}_2^{-1} \boldsymbol{K} \xi + O(1), \quad |\xi| \to \infty. \tag{8d}$$

An analytic solution to the above boundary value problem appears to be extremely difficult to obtain since we have to handle the boundary conditions on $\mathrm{Im}\{\xi\} = 0$, the interface conditions on $|\xi| = R^{1/2}$, $-\pi \le \arg\{\xi\} \le 0$, and those on $\xi \in L$.

Adding the two interface conditions in (8c), we arrive at

$$\boldsymbol{f}_2(\xi) = \boldsymbol{f}_3(\xi) - \xi^2 \begin{bmatrix} \varepsilon_{32}^* + \mathrm{i}\varepsilon_{31}^* \\ -\frac{1}{2}(E_2^* + \mathrm{i}E_1^*) \end{bmatrix} + \bar{\xi}^2 \begin{bmatrix} \varepsilon_{32}^* - \mathrm{i}\varepsilon_{31}^* \\ -\frac{1}{2}(E_2^* - \mathrm{i}E_1^*) \end{bmatrix}, \quad \xi \in L. \tag{9}$$

The region $\xi \in \Omega_3$ is simply connected if $z \in S_3$ is simply connected. Consequently, there exists a conformal mapping $\xi = w(\eta)$ that maps the exterior of the simply connected region Ω_3 in the ξ-plane onto the exterior of the unit circle $|\eta| \ge 1$ in the η-plane [Kantorovich and Krylov 1958; Savin 1961; England 1971]. As a result, an auxiliary function $D(\xi)$ can be constructed as follows:

$$\bar{\xi}^2 = \left[\bar{w}\left(\frac{1}{w^{-1}(\xi)}\right)\right]^2 = D(\xi), \quad \xi \in L, \tag{10}$$

where $w^{-1}(\xi)$ is the inverse mapping of $\xi = w(\eta)$.

Moreover, $D(\xi)$ is analytic in the exterior of Ω_3 except at the point at infinity, where it has a pole of finite degree, namely

$$D(\xi) \cong P(\xi) + O(\xi^{-1}), \quad |\xi| \to \infty, \tag{11}$$

where $P(\xi)$ is a polynomial of order $2N$ in ξ if $\xi = w(\eta)$ is a polynomial of order N in $1/\eta$.

Using (10) and (11), Equation (9) can be written as

$$\begin{aligned}\boldsymbol{f}_2(\xi) - [D(\xi) - P(\xi)]\begin{bmatrix}\varepsilon_{32}^* - \mathrm{i}\varepsilon_{31}^* \\ -\frac{1}{2}(E_2^* - \mathrm{i}E_1^*)\end{bmatrix} \\ = \boldsymbol{f}_3(\xi) - \xi^2\begin{bmatrix}\varepsilon_{32}^* + \mathrm{i}\varepsilon_{31}^* \\ -\frac{1}{2}(E_2^* + \mathrm{i}E_1^*)\end{bmatrix} + P(\xi)\begin{bmatrix}\varepsilon_{32}^* - \mathrm{i}\varepsilon_{31}^* \\ -\frac{1}{2}(E_2^* - \mathrm{i}E_1^*)\end{bmatrix}, \quad \xi \in L. \quad (12)\end{aligned}$$

In view of (12), we introduce a new analytic vector function $\boldsymbol{h}(\xi)$ defined by

$$\boldsymbol{h}(\xi) = \begin{cases} \boldsymbol{f}_2(\xi) - [D(\xi) - P(\xi)]\begin{bmatrix}\varepsilon_{32}^* - \mathrm{i}\varepsilon_{31}^* \\ -\frac{1}{2}(E_2^* - \mathrm{i}E_1^*)\end{bmatrix}, & \xi \in \Omega_2; \\ \boldsymbol{f}_3(\xi) - \xi^2\begin{bmatrix}\varepsilon_{32}^* + \mathrm{i}\varepsilon_{31}^* \\ -\frac{1}{2}(E_2^* + \mathrm{i}E_1^*)\end{bmatrix} + P(\xi)\begin{bmatrix}\varepsilon_{32}^* - \mathrm{i}\varepsilon_{31}^* \\ -\frac{1}{2}(E_2^* - \mathrm{i}E_1^*)\end{bmatrix}, & \xi \in \Omega_3. \end{cases} \quad (13)$$

We can see from the above definition and (12) that $\boldsymbol{h}(\xi)$ is continuous across $\xi \in L$ and is then analytic in $\xi \in \Omega_2 \cup \Omega_3$ except at the point at infinity, where its asymptotic behavior is the same as that of $\boldsymbol{f}_2(\xi)$ given by (8d).

By satisfying the boundary conditions on $\mathrm{Im}\{\xi\} = 0$ and the interface conditions on $|\xi| = R^{1/2}$, $-\pi \le \arg\{\xi\} \le 0$, using analytic continuation across straight and circular boundaries, we finally arrive at the following expressions for $\boldsymbol{f}_1(\xi)$, $\boldsymbol{f}_2(\xi)$, and $\boldsymbol{f}_3(\xi)$:

$$\begin{aligned}\boldsymbol{f}_1(\xi) = {} & 2(\boldsymbol{C}_1 + \boldsymbol{C}_2)^{-1}\boldsymbol{C}_2 \\ & \times\Bigg\{[D(\xi) - P(\xi)]\begin{bmatrix}\varepsilon_{32}^* - \mathrm{i}\varepsilon_{31}^* \\ -\frac{1}{2}(E_2^* - \mathrm{i}E_1^*)\end{bmatrix} \\ & \quad -[\overline{D}(\xi) - \overline{P}(x)]\begin{bmatrix}\varepsilon_{32}^* + \mathrm{i}\varepsilon_{31}^* \\ -\frac{1}{2}(E_2^* + \mathrm{i}E_1^*)\end{bmatrix} + \mathrm{i}\sqrt{\frac{2}{\pi}}\boldsymbol{C}_2^{-1}\boldsymbol{K}\xi\Bigg\}, \quad \xi \in \Omega_1; \quad (14)\end{aligned}$$

$$\begin{aligned}\boldsymbol{f}_2(\xi) = {} & (\boldsymbol{C}_1 + \boldsymbol{C}_2)^{-1}(\boldsymbol{C}_1 - \boldsymbol{C}_2) \\ & \times\Bigg\{[\overline{D}(R/\xi) - \overline{P}(R/\xi)]\begin{bmatrix}\varepsilon_{32}^* + \mathrm{i}\varepsilon_{31}^* \\ -\frac{1}{2}(E_2^* + \mathrm{i}E_1^*)\end{bmatrix} \\ & \quad - [D(R/\xi) - P(R/\xi)\begin{bmatrix}\varepsilon_{32}^* - \mathrm{i}\varepsilon_{31}^* \\ -\frac{1}{2}(E_2^* - \mathrm{i}E_1^*)\end{bmatrix} - \mathrm{i}\sqrt{\frac{2}{\pi}}\boldsymbol{C}_2^{-1}\boldsymbol{K}R\xi^{-1}\Bigg\} \\ & + [D(\xi) - P(\xi)]\begin{bmatrix}\varepsilon_{32}^* - \mathrm{i}\varepsilon_{31}^* \\ -\frac{1}{2}(E_2^* - \mathrm{i}E_1^*)\end{bmatrix} - [\overline{D}(\xi) - \overline{P}(\xi)]\begin{bmatrix}\varepsilon_{32}^* + \mathrm{i}\varepsilon_{31}^* \\ -\frac{1}{2}(E_2^* + \mathrm{i}E_1^*)\end{bmatrix} \\ & + \mathrm{i}\sqrt{\frac{2}{\pi}}\boldsymbol{C}_2^{-1}\boldsymbol{K}\xi, \qquad \xi \in \Omega_2; \quad (15)\end{aligned}$$

$$
\begin{aligned}
\boldsymbol{f}_3(\xi) = {} & (\boldsymbol{C}_1+\boldsymbol{C}_2)^{-1}(\boldsymbol{C}_1-\boldsymbol{C}_2) \\
& \times \left\{ [\overline{D}(R/\xi)-\overline{P}(R/\xi)] \begin{bmatrix} \varepsilon_{32}^*+\mathrm{i}\varepsilon_{31}^* \\ -\frac{1}{2}(E_2^*+\mathrm{i}E_1^*) \end{bmatrix} \right. \\
& \qquad \left. -[D(R/\xi)-P(R/\xi)] \begin{bmatrix} \varepsilon_{32}^*-\mathrm{i}\varepsilon_{31}^* \\ -\frac{1}{2}(E_2^*-\mathrm{i}E_1^*) \end{bmatrix} - \mathrm{i}\sqrt{\frac{2}{\pi}}\boldsymbol{C}_2^{-1}\boldsymbol{K}R\xi^{-1} \right\} \\
& + \xi^2 \begin{bmatrix} \varepsilon_{32}^*+\mathrm{i}\varepsilon_{31}^* \\ -\frac{1}{2}(E_2^*+\mathrm{i}E_1^*) \end{bmatrix} - P(\xi) \begin{bmatrix} \varepsilon_{32}^*-\mathrm{i}\varepsilon_{31}^* \\ -\frac{1}{2}(E_2^*-\mathrm{i}E_1^*) \end{bmatrix} \\
& - [\overline{D}(\xi)-\overline{P}(\xi)] \begin{bmatrix} \varepsilon_{32}^*+\mathrm{i}\varepsilon_{31}^* \\ -\frac{1}{2}(E_2^*+\mathrm{i}E_1^*) \end{bmatrix} + \mathrm{i}\sqrt{\frac{2}{\pi}}\boldsymbol{C}_2^{-1}\boldsymbol{K}\xi, \qquad \xi \in \Omega_3. \quad (16)
\end{aligned}
$$

It is not difficult to verify that the analytic vector functions obtained satisfy all the existing boundary and interface conditions as well as the required asymptotic behavior at infinity.

4. Stress and electric displacement intensity factors

The resultant stress and electric displacement intensity factors K_R^σ and K_R^D at the crack tip are defined by [Lee et al. 2000]

$$
K_R^\sigma = \lim_{x_1\to 0^+}[\sqrt{2\pi x_1}\sigma_{32}(x_1,0)], \quad K_R^D = \lim_{x_1\to 0^+}[\sqrt{2\pi x_1}D_2(x_1,0)], \qquad (17)
$$

or equivalently

$$
\boldsymbol{K}_R = \begin{bmatrix} K_R^\sigma \\ K_R^D \end{bmatrix} = \lim_{z\to 0}[\sqrt{2\pi z}\boldsymbol{C}_1\boldsymbol{f}_1'(z)]. \qquad (18)
$$

Using these definitions and (14), we ultimately obtain a concise and elegant expression of the resultant field intensity factors as

$$
\begin{aligned}
\boldsymbol{K}_R = {} & 2(\boldsymbol{C}_1^{-1}+\boldsymbol{C}_2^{-1})^{-1}\boldsymbol{C}_2^{-1}\boldsymbol{K} \\
& + 2\sqrt{2\pi}(C_1^{-1}+\boldsymbol{C}_2^{-2})^{-1}\mathrm{Im}\left\{ [D'(0)-P'(0)] \begin{bmatrix} \varepsilon_{32}^*-\mathrm{i}\varepsilon_{31}^* \\ -\frac{1}{2}(E_2^*-\mathrm{i}E_1^*) \end{bmatrix} \right\}. \quad (19)
\end{aligned}
$$

We can see from the above expression that the intensity factors are independent of the radius of the circular inhomogeneity. Moreover, we can deduce that when the eigenstrains and eigenelectric fields satisfy the condition

$$
\frac{\varepsilon_{31}^*}{\varepsilon_{32}^*} = \frac{E_1^*}{E_2^*} = \frac{\mathrm{Im}\{D'(0)-P'(0)\}}{\mathrm{Re}\{D'(0)-P'(0)\}}, \qquad (20)
$$

Equation (19) gives us that

$$
\boldsymbol{K}_R = 2(\boldsymbol{C}_1^{-1}+\boldsymbol{C}_2^{-1})^{-1}\boldsymbol{C}_2^{-1}\boldsymbol{K}, \qquad (21)
$$

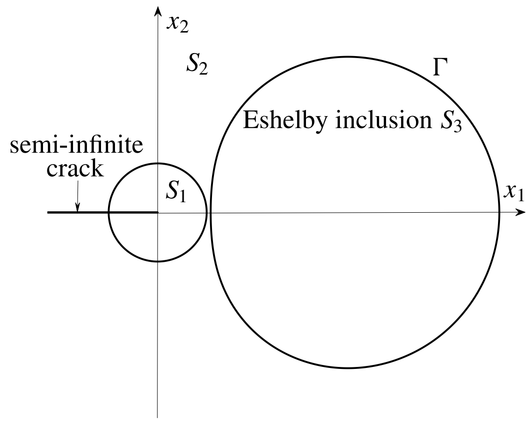

Figure 3. A noncircular interface Γ when $\xi \in L$ is circular.

which implies that the Eshelby inclusion exerts no influence on the resultant field intensity factors at the crack tip, or equivalently exerts a neutral effect on the electroelastic field at the crack tip. Note that the condition in (20) is independent of the electroelastic constants of the fibrous piezoelectric composite.

5. An illustrative example

In this example, $\xi \in L$ is a circle described by

$$|\xi - \xi_0| = d, \quad \xi \in L. \tag{22}$$

Although $\xi \in L$ is a circle, $z \in \Gamma$ is noncircular. Such a noncircular interface Γ is shown in Figure 3. The auxiliary function $D(\xi)$ and the polynomial $P(\xi)$ are found to be

$$D(\xi) = \frac{d^4}{(\xi - \xi_0)^2} + \frac{2\bar{\xi}_0 d^2}{\xi - \xi_0} + \bar{\xi}^2, \quad P(\xi) = \bar{\xi}^2. \tag{23}$$

Substituting these into (14)–(16), we obtain specific expressions for the three analytic vector functions as follows:

$$\begin{aligned} \boldsymbol{f}_1(\xi) = {} & 2(\boldsymbol{C}_1 + \boldsymbol{C}_2)^{-1}\boldsymbol{C}_2 \\ & \times \left\{ \left[\frac{d^4}{(\xi - \xi_0)^2} + \frac{2\bar{\xi}_0 d^2}{\xi - \xi_0} \right] \begin{bmatrix} \varepsilon_{32}^* - \mathrm{i}\varepsilon_{31}^* \\ -\frac{1}{2}(E_2^* - \mathrm{i}E_1^*) \end{bmatrix} \right. \\ & \quad - \left[\frac{d^4}{(\xi - \bar{\xi}_0)^2} + \frac{2\xi_0 d^2}{\xi - \bar{\xi}_0} \right] \begin{bmatrix} \varepsilon_{32}^* + \mathrm{i}\varepsilon_{31}^* \\ -\frac{1}{2}(E_2^* + \mathrm{i}E_1^*) \end{bmatrix} \\ & \quad \left. + \mathrm{i}\sqrt{\frac{2}{\pi}} \boldsymbol{C}_2^{-1} \boldsymbol{K} \xi \right\}, \qquad \xi \in \Omega_1; \end{aligned} \tag{24}$$

$$\begin{aligned}\boldsymbol{f}_2(\xi) &= (\boldsymbol{C}_1+\boldsymbol{C}_2)^{-1}(\boldsymbol{C}_1-\boldsymbol{C}_2)\\ &\quad\times\left\{\left[\frac{d^4}{(R\xi^{-1}-\bar{\xi}_0)^2}+\frac{2\xi_0 d^2}{R\xi^{-1}-\bar{\xi}_0}\right]\begin{bmatrix}\varepsilon_{32}^*+\mathrm{i}\varepsilon_{31}^*\\ -\frac{1}{2}(E_2^*+\mathrm{i}E_1^*)\end{bmatrix}\right.\\ &\qquad-\left[\frac{d^4}{(R\xi^{-1}-\xi_0)^2}+\frac{2\bar{\xi}_0 d^2}{R\xi^{-1}-\xi_0}\right]\begin{bmatrix}\varepsilon_{32}^*-\mathrm{i}\varepsilon_{31}^*\\ -\frac{1}{2}(E_2^*-\mathrm{i}E_1^*)\end{bmatrix}\\ &\qquad\left.-\mathrm{i}\sqrt{\frac{2}{\pi}}\boldsymbol{C}_2^{-1}\boldsymbol{K}R\xi^{-1}\right\}\\ &\quad+\left[\frac{d^4}{(\xi-\xi_0)^2}+\frac{2\bar{\xi}_0 d^2}{\xi-\xi_0}\right]\begin{bmatrix}\varepsilon_{32}^*-\mathrm{i}\varepsilon_{31}^*\\ -\frac{1}{2}(E_2^*-\mathrm{i}E_1^*)\end{bmatrix}\\ &\quad-\left[\frac{d^4}{(\xi-\bar{\xi}_0)^2}+\frac{2\xi_0 d^2}{\xi-\bar{\xi}_0}\right]\begin{bmatrix}\varepsilon_{32}^*+\mathrm{i}\varepsilon_{31}^*\\ -\frac{1}{2}(E_2^*+\mathrm{i}E_1^*)\end{bmatrix}+\mathrm{i}\sqrt{\frac{2}{\pi}}\boldsymbol{C}_2^{-1}\boldsymbol{K}\xi,\quad \xi\in\Omega_2;\end{aligned}\tag{25}$$

$$\begin{aligned}\boldsymbol{f}_3(\xi) &= (\boldsymbol{C}_1+\boldsymbol{C}_2)^{-1}(\boldsymbol{C}_1-\boldsymbol{C}_2)\\ &\quad\times\left\{\left[\frac{d^4}{(R\xi^{-1}-\bar{\xi}_0)^2}+\frac{2\xi_0 d^2}{R\xi^{-1}-\bar{\xi}_0}\right]\begin{bmatrix}\varepsilon_{32}^*+\mathrm{i}\varepsilon_{31}^*\\ -\frac{1}{2}(E_2^*+\mathrm{i}E_1^*)\end{bmatrix}\right.\\ &\qquad-\left[\frac{d^4}{(R\xi^{-1}-\xi_0)^2}+\frac{2\bar{\xi}_0 d^2}{R\xi^{-1}-\xi_0}\right]\begin{bmatrix}\varepsilon_{32}^*-\mathrm{i}\varepsilon_{31}^*\\ -\frac{1}{2}(E_2^*-\mathrm{i}E_1^*)\end{bmatrix}\\ &\qquad\left.-\mathrm{i}\sqrt{\frac{\pi}{2}}\boldsymbol{C}_2^{-1}\boldsymbol{K}R\xi^{-1}\right\}\\ &\quad+\xi^2\begin{bmatrix}\varepsilon_{32}^*+\mathrm{i}\varepsilon_{31}^*\\ -\frac{1}{2}(E_2^*+\mathrm{i}E_1^*)\end{bmatrix}-\bar{\xi}_0^2\begin{bmatrix}\varepsilon_{32}^*-\mathrm{i}\varepsilon_{31}^*\\ -\frac{1}{2}(E_2^*-\mathrm{i}E_1^*)\end{bmatrix}\\ &\quad-\left[\frac{d^4}{(\xi-\bar{\xi}_0)^2}+\frac{2\xi_0 d^2}{\xi-\bar{\xi}_0}\right]\begin{bmatrix}\varepsilon_{32}^*+\mathrm{i}\varepsilon_{31}^*\\ -\frac{1}{2}(E_2^*+\mathrm{i}E_1^*)\end{bmatrix}+\mathrm{i}\sqrt{\frac{2}{\pi}}\boldsymbol{C}_2^{-1}\boldsymbol{K}\xi,\quad \xi\in\Omega_3.\end{aligned}\tag{26}$$

Substituting (23) into (19) yields

$$\begin{aligned}\boldsymbol{K}_R &= 2(\boldsymbol{C}_1^{-1}+\boldsymbol{C}_2^{-1})^{-1}\boldsymbol{C}_2^{-1}\boldsymbol{K}\\ &\quad+\frac{2\sqrt{2\pi}d^2(|\xi_0|^2-d^2)}{|\xi_0|^6}(\boldsymbol{C}_1^{-1}+\boldsymbol{C}_2^{-1})^{-1}\\ &\quad\times\begin{bmatrix}2[\varepsilon_{31}^*u_0(u_0^2-3v_0^2)+\varepsilon_{32}^*v_0(3u_0^2-v_0^2)]\\ -E_1^*u_0(u_0^2-3v_0^2)-E_2^*v_0(3u_0^2-v_0^2)\end{bmatrix},\end{aligned}\tag{27}$$

where

$$\begin{aligned}u_0 &= \mathrm{Re}\{\xi_0\},\\ v_0 &= \mathrm{Im}\{\xi_0\}.\end{aligned}\tag{28}$$

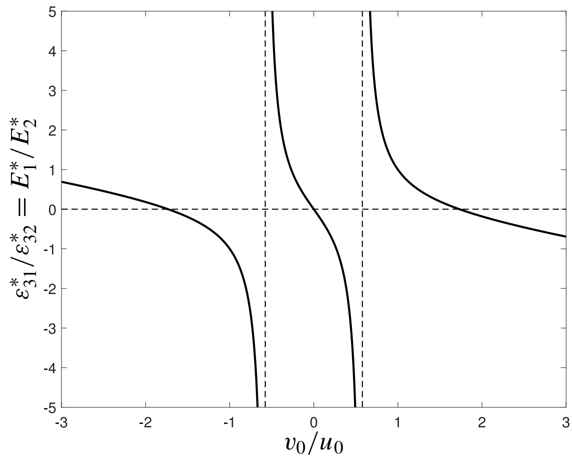

Figure 4. Variation of $\varepsilon_{31}^*/\varepsilon_{32}^* = E_1^*/E_2^*$ as a function of v_0/u_0 in (29).

When the eigenstrains and eigenelectric fields satisfy

$$\frac{\varepsilon_{31}^*}{\varepsilon_{32}^*} = \frac{E_1^*}{E_2^*} = \frac{v_0(v_0^2 - 3u_0^2)}{u_0(u_0^2 - 3v_0^2)}, \tag{29}$$

the inclusion will have no influence on the resultant field intensity factors at the crack tip. Condition (29) can be deduced from (20) or indeed from (27). The variation of $\varepsilon_{31}^*/\varepsilon_{32}^* = E_1^*/E_2^*$ as a function of v_0/u_0 in (29) is illustrated in Figure 4. It is seen in Figure 4 that $\varepsilon_{31}^* = E_1^* = 0$ when $v_0/u_0 = \pm\sqrt{3} = \pm 1.7321$ and that $\varepsilon_{32}^* = E_2^* = 0$ when $v_0/u_0 = \pm 1/\sqrt{3} = \pm 0.5774$.

Due to the fact that $\xi \in \Omega_3$ is circular, the average stresses and electric displacements within the Eshelby inclusion can be determined as

$$\begin{aligned}
\begin{bmatrix} \langle \sigma_{32} + \mathrm{i}\sigma_{31} \rangle \\ \langle D_2 + \mathrm{i} D_1 \rangle \end{bmatrix}
&= -\mathrm{i}\sqrt{\frac{1}{2\pi}} \boldsymbol{K} \xi_0^{-1} - \boldsymbol{C}_2 \left[1 + \frac{d^2(d^2 - |\xi_0|^2 + \xi_0^2)}{\xi_0(\xi_0 - \bar{\xi}_0)^3} \right] \begin{bmatrix} \varepsilon_{32}^* + \mathrm{i}\varepsilon_{31}^* \\ -\frac{1}{2}(E_2^* + \mathrm{i}E_1^*) \end{bmatrix} \\
&\quad + \boldsymbol{C}_2 (\boldsymbol{C}_1 + \boldsymbol{C}_2)^{-1} (\boldsymbol{C}_2 - \boldsymbol{C}_1) \\
&\quad \times \left\{ \frac{d^2 R (d^2 + R - |\xi_0|^2)}{(R - |\xi_0|^2)^3} \begin{bmatrix} \varepsilon_{32}^* + \mathrm{i}\varepsilon_{31}^* \\ -\frac{1}{2}(E_2^* + \mathrm{i}E_1^*) \end{bmatrix} \right. \\
&\qquad - \frac{d^2 R [\xi_0 (d^2 - |\xi_0|^2) + \bar{\xi}_0 R]}{\xi_0 (R - \xi_0^2)^3} \begin{bmatrix} \varepsilon_{32}^* - \mathrm{i}\varepsilon_{31}^* \\ -\frac{1}{2}(E_2^* - \mathrm{i}E_1^*) \end{bmatrix} \\
&\qquad \left. + \mathrm{i}\sqrt{\frac{1}{2\pi}} \boldsymbol{C}_2^{-1} \boldsymbol{K} R \xi_0^{-3} \right\},
\end{aligned} \tag{30}$$

where $\langle \cdot \rangle$ denotes the average over $\xi \in \Omega_3$.

6. Conclusions

We present a general method leading to an analytic solution of the interaction problem of an Eshelby inclusion of arbitrary shape undergoing uniform antiplane eigenstrains and in-plane eigenelectric fields near a circular piezoelectric inhomogeneity partially penetrated by a semi-infinite crack. The cracked piezoelectric plane in the physical z-plane is mapped onto the lower half of the image plane via the conformal mapping in (7). An auxiliary function $D(\xi)$ is constructed in (10). With the aid of $D(\xi)$, we apply analytic continuations across the straight boundary $\mathrm{Im}\{\xi\} = 0$ and across the circular boundary $|\xi| = R^{1/2}$ to arrive at the three analytic vector functions $\boldsymbol{f}_1(\xi)$, $\boldsymbol{f}_2(\xi)$, and $\boldsymbol{f}_3(\xi)$. A concise and elegant expression of the resultant stress and electric displacement intensity factors at the crack tip is obtained in (19). As an illustrative example, we present explicit expressions of the three analytic vector functions and the resultant intensity factors for the special case when $\xi \in L$ is a circle.

Acknowledgements

This work is supported by a grant from the National Natural Science Foundation of China (No. 11272121) and a Discovery Grant from the Natural Sciences and Engineering Research Council of Canada (RGPIN — 2017 - 03716115112).

References

[Chung and Ting 1996] M. Y. Chung and T. C. T. Ting, "Piezoelectric solid with an elliptic inclusion or hole", *Int. J. Solids Struct.* **33** (1996), 3343–3361.

[Deeg 1980] W. F. Deeg, *The analysis of dislocation, crack, and inclusion problems in piezoelectric solids*, Ph.D. thesis, Stanford University, Stanford, CA, 1980.

[England 1971] A. H. England, *Complex variable methods in elasticity*, Wiley, London, 1971.

[Kantorovich and Krylov 1958] L. V. Kantorovich and V. I. Krylov, *Approximate methods in higher analysis*, Interscience, New York, 1958.

[Kuo and Barnett 1991] C. M. Kuo and D. M. Barnett, "Stress singularities of interfacial cracks in bonded piezoelectric half-spaces", pp. 33–50 in *Modern theory of anisotropic elasticity and applications* (Research Triangle Park, NC, 1990), edited by J. J. Wu et al., 1991.

[Lee et al. 2000] K. Y. Lee, W. G. Lee, and Y. E. Pak, "Interaction between a semi-infinite crack and a screw dislocation in a piezoelectric material", *J. Appl. Mech.* (*ASME*) **67** (2000), 165–170.

[Pak 1990] Y. E. Pak, "Crack extension force in a piezoelectric material", *J. Appl. Mech.* (*ASME*) **57** (1990), 647–653.

[Ru 2000] C. Q. Ru, "Eshelby's problem for two-dimensional piezoelectric inclusions of arbitrary shape", *Proc. R. Soc. Lond. A* **456**:1997 (2000), 1051–1068.

[Ru 2001] C. Q. Ru, "A two-dimensional Eshelby problem for two bonded piezoelectric half-planes", *Proc. R. Soc. Lond. A* **457**:2008 (2001), 865–883.

[Savin 1961] G. N. Savin, *Stress concentration around holes*, Pergamon Press, London, 1961.

[Suo et al. 1992] Z. Suo, C. M. Kuo, D. M. Barnett, and J. R. Willis, "Fracture mechanics for piezoelectric ceramics", *J. Mech. Phys. Solids* **40** (1992), 739–765.

[Wang and Fan 2015] X. Wang and H. Fan, "A piezoelectric screw dislocation in a bimaterial with surface piezoelectricity", *Acta Mech.* **226** (2015), 3317–3331.

[Wang and Schiavone 2017] X. Wang and P. Schiavone, "Debonded arc-shaped interface conducting rigid line inclusions in piezoelectric composites", *Comptes Rendus Méc.* **345**:10 (2017), 724–731.

Received 3 Nov 2017. Revised 9 Jan 2018. Accepted 17 Feb 2018.

XU WANG: xuwang@ecust.edu.cn
School of Mechanical and Power Engineering, East China University of Science and Technology, Shanghai, China

PETER SCHIAVONE: p.schiavone@ualberta.ca
Department of Mechanical Engineering, University of Alberta, Edmonton, AB, Canada